Chemical Engineering Science 65 (2010) 4194–4207

Contents lists available at ScienceDirect

Chemical Engineering Science

journal homepage: www.elsevier.com/locate/ces

A cubic equation of state based on saturated vapor modeling and the application of model-based design of experiments for its validation

Alexander Kud [a,*], Stefan Körkel [b], Stefan Maixner [a]

[a] Division of Research at BASF SE, BASF SE, Carl-Bosch-Straße 38, 67056 Ludwigshafen, Germany
[b] Interdisciplinary Center for Scientific Computing at Ruprecht-Karls-University of Heidelberg, Germany

ARTICLE INFO

Article history:
Received 20 July 2009
Received in revised form
3 March 2010
Accepted 19 April 2010
Available online 22 April 2010

Keywords:
Kinetics
Phase equilibria
Cubic equation of state (CEoS)
Soave–Redlich–Kwong (SRK)
Peng–Robinson (PR)
Model-based design of experiments
Model validation
Parameter identification
Optimization

ABSTRACT

For simulation of chemical processes, a sufficiently accurate mathematical description of phase equilibria is essential. In order to achieve this, high-quality measured data and model equations are indispensable. A new gamma-function as a replacement for the common alpha-function in cubic equations of state is proposed here for polar compounds with an existing vapor phase. The equation parameters of the gamma-function are fitted to state data on the dew line instead of, as usual, on the vaporization curve. The quality of the description is compared to the customary equations of state using statistical parameters. A further validation used for the description is the prediction of caloric parameters and the comparison thereof with measured data. By means of model-based experimental design, the gamma-function and the equation of state based thereon are validated. Multiple setpoint optimization allows a uniform experimental design for validation of a vapor pressure equation and of a vapor density equation to be calculated for polar compounds. The experiments calculated optimally in this way reduce large test series to a few experiments which are significant for the specific model equation.

1. Introduction

Cubic equations of state (CEoS) have been used successfully for the modeling of the vapor–liquid equilibrium (VLE) for many years. For historical reasons, the fields of use were at first restricted to the hydrocarbons. In the last few years, the equations have increasingly also been improved for other substance classes. The emphasis of the further development of the CEoS was a better description of the liquid density and the composition of the phases.

In a kinetic modeling of reactions in a vapor–liquid system, the task was to monitor and quantitatively model the kinetics in the liquid phase via a pressure measurement. In order to be able to determine the concentrations in the liquid phase with sufficient accuracy, it is necessary that the mass balance in the particular phase and hence the density thereof are described sufficiently accurately. Experience has shown that the relative error in the density modeling should not exceed 1–2%. Systematic density errors are projected into these parameters in the estimation of the kinetic parameters. As a result, activation energies and frequency factors gain considerable systematic deviations. It can be shown that in the case of gas metering at the start of the reaction and in the case of gas evolution during the reaction, it is advantageous for the accuracy of the kinetic parameters when a considerable gas volume is present compared to the liquid phase. This gas volume has the function of a reservoir, to which a reactant which forms in the liquid phase can be released or taken up again therefrom. When this vaporous reservoir is too small compared to the liquid phase, the reaction stops, and hence the kinetic parameters can be estimated only with large variances, if at all. The consequence is that the kinetic model cannot be validated.

In order that the relevant error of 1–2% in the density modeling is not exceeded for the polar system that we are using, we decided to adopt the $\gamma-\varphi-$approach. This allows both phases to be described with separate density equations. For our VLE modeling, a greater density range is needed, and a cubic equation of state was therefore selected to describe the vapor phase. For the less polar hydrocarbons, the $\varphi-\varphi-$approach is suitable, because the vapor density, just like the liquid density, is described very well with the same CEoS, as also shown by Smith et al. (2005, p. 99). Among the CEoS, for example, the Soave–Redlich–Kwong (SRK) and the Peng–Robinson (PR) equations have found many applications. For this reason, we would like to restrict ourselves in this study to these two cubic equations of state.

Since the reactions in the liquid phase are monitored by means of a pressure measurement in the vapor phase, and since the

* Corresponding author. Tel.: +49 621 40 7 12.
E-mail address: Alexander.Kud@basf.com (A. Kud).

0009-2509/$ - see front matter © 2010 Elsevier Ltd. All rights reserved.
doi:10.1016/j.ces.2010.04.025

proportion of the vapor phase cannot be disregarded for the kinetic measurements, we studied the CEoS with regard to the vapor density description for polar compounds. A prerequisite for a good description of mixtures is a good description of the pure substance properties with the selected equation of state. We therefore concentrate in this study first on the pure compounds. We would like to point out here that we distinguish the gaseous state and the vaporous state. The vaporous state is a special form of the gas phase which must always coexist in a state of equilibrium together with a liquid phase. In the following text all state variables and parameters relating to the phase equilibrium are in bold type.

In the SRK and PR equations

$$p_M = \frac{RT}{\upsilon - b_M} - \frac{a_{c,M} \cdot \alpha(T)}{(\upsilon + \delta_M b_M) \cdot (\upsilon + \varepsilon_M b_M)}, \tag{1}$$

the vapor pressure correction for a pure substance is undertaken by means of the alpha-function $\alpha(T)$ in the attraction term, where p_M is the calculated pressure and $a_{c,M}, b_M, \delta_M, \varepsilon_M$ are the model parameters according to the approach. They can be found in Appendix A. The correction function $\alpha(T)$ used here is the frequently cited equation according to Soave (1972).

With knowledge of the temperature-dependent vapor pressure description, this equation can be used to calculate the molar volume of the vapor phase and hence the vapor density. Fig. 1 shows, for the three polar substances sulfur dioxide, hydrogen chloride and ammonia, the difference of calculated vapor density and the vapor density figures of the literature.

For all three compounds studied, the vapor density is calculated systematically too low within the range of $0.6 \le T_r \le 0.9$. For higher temperatures, the systematic error becomes even greater, since the SRK and PR equations do not correctly describe the critical vapor density owing to the critical compressibility factor which is constant in each case. In the case of phase equilibrium modeling, the vapor density error leads to an equally high mass balance error. In this context we investigated the correction function according to the MSRK equation (Soave, 1979). The parameters m and n in the MSRK equation are unique for every compound and the vapor pressure is much better described with two parameters. Sandurasi et al. (1986) published the specific parameters for the compounds which we investigated in this work. The calculations lead to the same deviations in the vapor densities as can be seen in Fig. 1.

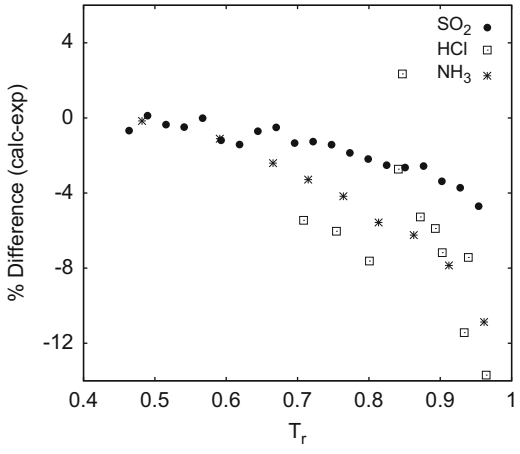

Fig. 1. Percentage deviation between the calculated density based on the SRK equation and the density from the literature figures (partly measured data). The scatter for HCl (~2.5%) is based on different literature sources for the vapor densities.

The aim of the studies presented here is to find an improved vapor and gas density description for polar compounds, though we do not wish to explicitly model the molecular properties, e.g. the influence of the dipole moment. The improvement is to be achieved by modeling on the dew line. This description is to find use in VLE modeling based on a $\gamma-\varphi-$approach. Moreover, the extent to which the model-based experimental design is suitable in the field of thermodynamics of phase equilibria for saving measurements and for designing the experiments optimally for model validation is to be examined. The model compound used for the studies was essentially ammonia, since there are very many reliable experimental data therefore.

2. Database

For the modeling of the equations of state, tabulated vapor pressure and vapor density data of ammonia from the VDI-Wärmeatlas (2002, Dcb 2) were used. The values reported there originate from a fundamental equation of Tillner-Roth et al. (1993), and also Baehr and Tillner-Roth (1995). Measured data of the gas state (pVT data) of ammonia originate from Meyers and Jessup (1925), and from Beattie and Lawrence (1930). The measured values reported were adopted as described. For the calculation of statistical evaluation parameters, the standard deviation or the relative measurement error is used for measurement data. The relative error of the pressure measurement for ammonia is 0.155% for the data of Meyers and Jessup, and 0.08% for those of Beattie and Lawrence.

For the subcritical state of ammonia, the parameters of the CEoS were determined by means of parameter estimation on the basis of the vapor pressure and vapor density data from the VDI-Wärmeatlas. The data on the dew line were thus used. For the pressure, a relative error of 0.2% ($v_p = 0.002$) and, to calculate the standard deviation, the following equation was used:

$$s_p = p_m \cdot v_p + 5 \times 10^{-3} \text{ bar}. \tag{2}$$

The offset of 5×10^{-3} bar has the meaning of a lower limit for the identifiability of a pressure measurement, which was set here at 5 mbar. The value of the offset correlates with the random noise of the apparatus in the lower measurement region. A realistic mean value was chosen which is oriented at the state of the art for measurement of the vapor pressure and of the vapor density. For the vapor density, a relative error of 0.5% ($v_\varrho = 0.005$), and the standard deviation was calculated according to

$$s_\varrho = \varrho_m \cdot v_\varrho + 1 \times 10^{-2} \text{ kg/m}^3. \tag{3}$$

For the parameter estimation, the vapor pressure and vapor density residuals were weighted with the standard deviation. The SRK and PR equations were checked and compared using pVT measured data of the gas state from Beattie and Meyers. For the checking of a consistent thermodynamic description of the two cubic equations of state, measured data of the specific heat capacity C_p according to figures from Barthau and Sohns (1974) and calculated data from the VDI-Wärmeatlas (2002, Dcb 2) based on the fundamental equation were employed for the vaporous state.

For the supercritical state of ammonia, the parameter values of the CEoS were fitted to the tabulated data of the fundamental equation from the VDI-Wärmeatlas (2002, Dbf 5). The examination is likewise done with measured data of Beattie and Meyers. In our study, the following critical constants of ammonia are used: $T_c = 405.55$ K, $p_c = 112.8$ bar, $V_c = 7.256 \times 10^{-5}$ m^3/mol (VDI-Wärmeatlas, 2002, Dcb 2; Barthau and Sohns, 1974), $T_p = 195.48$ K (triple-point temperature) (Ahrendts and Baehr, 1979, p. 9).

The substance-specific data for further polar compounds used in this study can be found in Appendix D.

3. Z modeling for the vapor

The introduction discussed the fact that the correction function $\alpha(T)$ for the vapor pressure has a crucial influence on the vapor density calculation which is inadequate for the compounds studied here. Poling et al. (2001, Chapter 4.20, Tables 4–7) give a very comprehensive overview of the different alpha-functions. Twu et al. (1991, 2002) described a new three-parameter alpha-function which is very suitable for non-polar and polar compounds.

When only the gaseous and vaporous state are of interest for the modeling, it is possible to fit the alpha-function in Eq. (1) directly to gas density measurements in the subcritical temperature range. Extrapolation to the vapor pressure of the dew line would allow the vapor density to be calculated. Whether this simple procedure is possible will be checked using the polar compound hydrogen chloride as example. The correction function used was the equation

$$\alpha(T_r)=\exp\left[\hat{\Theta}_{\alpha 1}\cdot\left(1-\frac{1}{T_r}\right)+\hat{\Theta}_{\alpha 2}\cdot\ln(T_r)+\hat{\Theta}_{\alpha 3}\cdot(T_r-1)\right],$$
$$\hat{\Theta}_{\alpha}=(\hat{\Theta}_{\alpha 1},\hat{\Theta}_{\alpha 2},\hat{\Theta}_{\alpha 3})^{\top}\in\mathbb{R}^3,\ T_r\in\mathbb{R}^+ \tag{4}$$

which has been found to be very good for many compounds over a wide temperature range. The database for the gas densities originates from Ahlberg (1985). The estimated parameters can be found in Table 1.

Together with Eq. (1), the rearranged DIPPR (Design Institute for Physical Properties) vapor pressure equation

$$\hat{\boldsymbol{p}}=p_c\cdot\exp\left[\frac{\hat{\boldsymbol{\Theta}}_{p1}}{T_c}\cdot\left(1-\frac{1}{\boldsymbol{T}_r}\right)+\hat{\boldsymbol{\Theta}}_{p2}\cdot\ln(\boldsymbol{T}_r)+\hat{\boldsymbol{\Theta}}_{p3}\cdot T_c^{\boldsymbol{\Theta}_{p4}}(\boldsymbol{T}_r^{\boldsymbol{\Theta}_{p4}}-1)\right],$$
$$(\hat{\boldsymbol{\Theta}}_{p1},\hat{\boldsymbol{\Theta}}_{p2},\hat{\boldsymbol{\Theta}}_{p3})^{\top}\in\mathbb{R}^3,\ \boldsymbol{\Theta}_{p4}\in\mathbb{N} \tag{5}$$

is used to calculate the vapor density, see Appendix D. The corresponding estimated parameters $\hat{\boldsymbol{\Theta}}_p$ for HCl are based on measured data in the reference work by Landold-Börnstein (1960, p. 189), from the VDI-Wärmeatlas (2002, Dca 1, Dcb 6) and Perry's Chemical Engineers' Handbook (Perry and Green, 1997, Chapter 2.58, Table 2.7), and can be found in Appendix D. In spite of fitting to the gas state, the differences between calculated and experimental data are −16% to 4% (Table 2) for both equations of state, which is too large for kinetic modeling. The reason is most probably a too large difference between the measured gas densities and the vapor densities. Therefore we would like to pursue and study modeling on the dew line employing a good description of the gas state.

Table 1
Parameters for the α correction function in Eq. (4) for the gaseous state of HCl.

Parameter	SRK	PR
$\hat{\Theta}_{\alpha 1}$	0.588428	32.9086
$\hat{\Theta}_{\alpha 2}$	−1.31091	−79.6647
$\hat{\Theta}_{\alpha 3}$	−0.271181	47.1005

Table 2
The absolute vapor density deviation between model and measurement for the case of a parameter assignment of the alpha-function in the subcritical gas state for HCl is calculated according to $(\varrho_M-\varrho_m)/\varrho_m\times 100\%$.

Absolute deviation (%)		
T_r	SRK	PR
0.708	−5.6	−6.0
0.755	−5.7	−5.8
0.801	−6.7	−7.0
0.847	4.0	2.8
0.893	−3.7	−6.3
0.939	−4.5	−9.1
0.841	−1.2	−2.2
0.872	−3.4	−5.2
0.903	−4.9	−7.8
0.934	−8.7	−12.9
0.964	−10.5	−15.8

Calculated vapor densities (kg/m^3) according to Eqs. (1), (4) and (5).

3.1. Expansion of the compressibility factor for the vapor

The compressibility factor Z can be represented as a function of the temperature, of the molar volume υ or of the pressure, and of the parameters of the molecular interaction Θ_Z. For the expansions required here, the compressibility factor is described as a function of temperature and of molar volume according to

$$Z=f_z(\upsilon,T,\Theta_Z),\quad \Theta_Z\in\mathbb{R}^n,\ \upsilon,T\in\mathbb{R}^+. \tag{6}$$

For a pure compound in a vapor–liquid equilibrium, according to the phase rule, only the equilibrium temperature $\boldsymbol{T}$ determines the vapor pressure $\boldsymbol{p}=\boldsymbol{f}_p(\boldsymbol{T})$. The molar vapor volume υ, just like the vapor pressure, thus depends only on the temperature

$$\upsilon=f_\upsilon(\boldsymbol{p},\boldsymbol{T})=f_\upsilon(\boldsymbol{f}_p(\boldsymbol{T}),\boldsymbol{T})=\boldsymbol{f}_\upsilon(\boldsymbol{T}). \tag{7}$$

The compressibility factor for the dew line $\boldsymbol{Z}$ can thus also be written as

$$\boldsymbol{Z}=f_z(\upsilon,\boldsymbol{T},\Theta_Z)=f_z(\boldsymbol{f}_\upsilon(\boldsymbol{T}),\boldsymbol{T},\Theta_Z)=\boldsymbol{f}_z(\boldsymbol{T},\Theta_Z). \tag{8}$$

The compressibility factor for the vapor is therefore now only temperature-dependent. The function $\boldsymbol{f}_z(\boldsymbol{T},\Theta_Z)$ can be expanded within the temperature range of $[\boldsymbol{T_p}\le\boldsymbol{T}_0<T_c]$ at the point $\boldsymbol{T}_0$ as the Taylor series

$$\boldsymbol{f}_z(\boldsymbol{T},\Theta_Z)=\sum_{k=0}^{\infty}\frac{(\boldsymbol{T}-\boldsymbol{T}_0)^k}{k!}\cdot\left(\frac{d^k\boldsymbol{f}_z(\boldsymbol{T},\Theta_Z)}{d\boldsymbol{T}^k}\right)_{T_0}. \tag{9}$$

When the term $(\boldsymbol{T}-\boldsymbol{T}_0)^k$ is expanded by the binomial theorem, a pure polynomial in $\boldsymbol{T}$ is obtained for $\boldsymbol{f}_z(\boldsymbol{T},\Theta_Z)$. When $\boldsymbol{T}_0$ is equal to the triple-point temperature $\boldsymbol{T_p}$, the pressure and the vapor density are very low for many compounds, such that there is almost ideal gas behavior and, for the 1st coefficient in Eq. (9):

$$\boldsymbol{f}_z(\boldsymbol{T_p},\Theta_Z)\approx 1. \tag{10}$$

In this case, $\tilde{\boldsymbol{f}}_z(\boldsymbol{T},\Theta_Z)$ is intended to be an approximation of $\boldsymbol{f}_z(\boldsymbol{T},\Theta_Z)$. Employing the binomial theorem, one obtains

$$\tilde{\boldsymbol{f}}_z(\boldsymbol{T},\Theta_Z)=1+\sum_{k=1}^{n}\left[\frac{1}{k!}\cdot\left(\frac{d^k\boldsymbol{f}_z(\boldsymbol{T},\Theta_Z)}{d\boldsymbol{T}^k}\right)_{T_{T_p}}\cdot\sum_{i=0}^{k}\binom{k}{i}\boldsymbol{T}^{k-i}(-\boldsymbol{T_p})^i\right]. \tag{11}$$

This equation is to serve as the basis for description of the vapor density by means of $\boldsymbol{Z}$ modeling. The function $\tilde{\boldsymbol{f}}_z(\boldsymbol{T},\Theta_Z)$ is not an equation of state in the general sense. The difference of our approach (9) or (11) to the virial equation, which is based on a similar approach, is described in Appendix B. The molecular interaction parameters are described by the temperature deviations (polynomial coefficients) in a semi-empirical kind. More details concerning the Z expansion and molecular interactions are in the text book by Prausnitz et al. (1999, Chapter 4.12) and Walas (1985, Chapter 1). How to get the molecular interaction parameters is described in the following.

3.2. The "experimental" compressibility factor for the vapor

In the same way as the vapor pressure is a characteristic property of a compound, this is also true for the vapor density and of course for the temperature-dependent compressibility factor of the dew line calculated therefrom. Vapor pressure and vapor density measurements can be used to determine an estimator function $\hat{\boldsymbol{Z}}$ for $\hat{\boldsymbol{f}}_z(\boldsymbol{T},\Theta_Z)$. To this end, we use the general definition of the compressibility factor for the vapor state

$$\boldsymbol{Z} := \frac{\boldsymbol{p}\upsilon}{\mathcal{R}\boldsymbol{T}} = \frac{\boldsymbol{p}}{\varrho^*\mathcal{R}\boldsymbol{T}} = \frac{\boldsymbol{p}T_c}{\varrho^*\mathcal{R}\boldsymbol{T}_r} \quad \text{with } \boldsymbol{T}_r = \boldsymbol{T}/T_c, \tag{12}$$

where $\boldsymbol{p}$ is the vapor pressure and ϱ^* is the molar vapor density. When the empirical estimator function (5) is selected for the vapor pressure and the estimator function $\hat{\boldsymbol{Z}}$ for the compressibility factor $\boldsymbol{Z}$, the measured vapor densities ϱ_m where $\varrho = \mathcal{M}/\upsilon$ can be estimated according to the equation

$$\hat{\varrho} = \frac{\mathcal{M}\hat{\boldsymbol{p}}}{\hat{\boldsymbol{Z}}\mathcal{R}\boldsymbol{T}} = \frac{\mathcal{M}p_c}{\mathcal{R}T_c}\cdot\frac{\hat{\boldsymbol{p}}_r}{\hat{\boldsymbol{Z}}\boldsymbol{T}_r}. \tag{13}$$

The estimator function $\hat{\boldsymbol{Z}}$ must satisfy the following criteria for the domain of definition: for low temperatures, there is approximately ideal behavior, which means that the compressibility factor is almost 1:

$$\lim_{T_r\to T_{p_r}} \hat{\boldsymbol{Z}} = a_1,\ a_1 \approx 1, \quad \boldsymbol{T}_r \in \left[\frac{T_p}{T_c},1\right]. \tag{14}$$

The temperature derivation at this point should be almost zero:

$$\lim_{T_r\to T_{p_r}} \frac{d\hat{\boldsymbol{Z}}}{d\boldsymbol{T}_r} = a_2, \quad a_2 \approx 0. \tag{15}$$

For the critical temperature, the critical real gas factor has to be calculated

$$\lim_{T_r\to 1} \hat{\boldsymbol{Z}} = Z_c. \tag{16}$$

The temperature derivative $d\hat{\boldsymbol{Z}}/d\boldsymbol{T}_r$ for $T_r \to 1$ must tend to $\to -\infty$. In practice, however, small values are sufficient, since this is not the critical range that is to be described here.

Based on the Z modeling (11), according to our experience, the following approach has been found to be good for the estimator $\hat{\boldsymbol{Z}}$:

$$\hat{\boldsymbol{Z}}_M = 1-(1-Z_{c,M})\cdot[\hat{\boldsymbol{\Theta}}_{Z1}\cdot\boldsymbol{T}_r^{q_1} + \hat{\boldsymbol{\Theta}}_{Z2}\cdot\boldsymbol{T}_r^{q_2} + \hat{\boldsymbol{\Theta}}_{Z3}\cdot\boldsymbol{T}_r^{q_3} + \hat{\boldsymbol{\Theta}}_{Z4}\cdot\boldsymbol{T}_r^{\hat{q}_4}],$$
$$\hat{\boldsymbol{\Theta}}_Z \in \mathbb{R}^4, \quad q_i \in \mathbb{N}\backslash\{1\}. \tag{17}$$

The parameter $\hat{\boldsymbol{\Theta}}_Z$ correlates with the polynomial coefficients $(d^k\boldsymbol{f}_z(\boldsymbol{T},\Theta_Z)/d\boldsymbol{T}^k)_{T_0}$ in Eq. (9) which describes the molecular interactions. Our experience in practice showed additional correlation for the parameters

$$\hat{\boldsymbol{\Theta}}_{Z4} = 1-\hat{\boldsymbol{\Theta}}_{Z1}-\hat{\boldsymbol{\Theta}}_{Z2}-\hat{\boldsymbol{\Theta}}_{Z3}, \tag{18}$$

$$\boldsymbol{q}_2 = \hat{\boldsymbol{q}}_4 - 1. \tag{19}$$

It should be mentioned that the proposed modeling according to (17)–(19) is mathematically not completely exhausted. The fundamental idea in this study is modeling on the dew line. To test this mathematical approach the parameters are determined from vapor pressure and vapor density measurements and the results for the five compounds with the same model approach are shown in Table 3. The exponent $\boldsymbol{q}_1$ describes the range close to the critical point and will be fixed to a value of 200 to met the condition of the temperature derivative $d\hat{\boldsymbol{Z}}/d\boldsymbol{T}_r$. If the region around the critical point is to be described more accurately, more measured points in this temperature range have to be collected. Our semi-empirical model approach describes the compressibility factor of the dew line from the triple point to $\boldsymbol{T}_r \le 0.96$ with only three estimated parameters from the vapor density measurements and the usually known vapor pressure function.

Table 3
Estimated parameters for the compressibility factor of various compounds.

	NH_3	HCl	SO_2	C_6H_5Cl	CH_3COCH_3
$\hat{\boldsymbol{q}}_4$	5	6	5	5	2
$\hat{\boldsymbol{\Theta}}_{Z1}$	0.186608	0.169379	0.217011	0.229046	0.350364
$\hat{\boldsymbol{\Theta}}_{Z2}$	−0.294962	0.66127	−0.494356	−0.697602	−1.38802
Scope for T_r	0.48–0.96	0.7–0.95	0.46–0.96	0.59–0.93	0.66–0.94

The basis is the model approach (13), (17)–(19) and $\boldsymbol{q}_1 = 200$, $\hat{\boldsymbol{\Theta}}_{Z3} = 0$. The basis is $\boldsymbol{Z}_{cm}$.

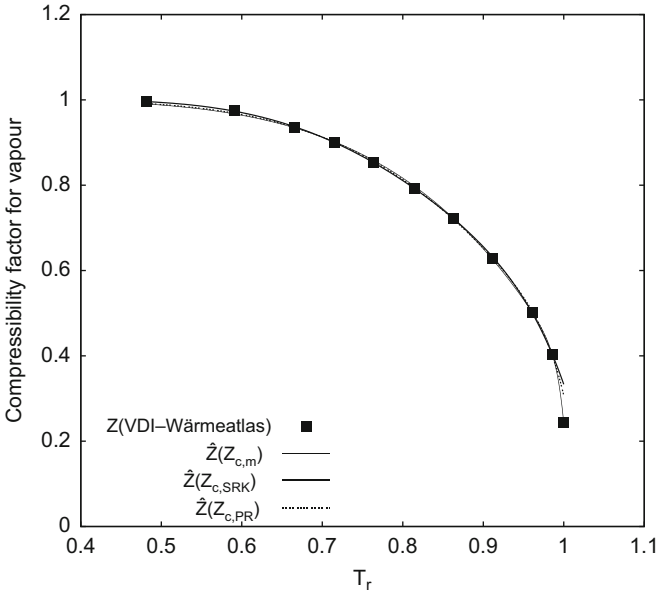

Fig. 2. Dependence of the compressibility factor on the temperature for NH_3 vapor. (Reduced triple point temperature $\boldsymbol{T}_{p_r} = 0.48$.)

The properties of ammonia with regard to $\boldsymbol{Z}$ modeling will be studied hereinafter. The values for $\hat{\boldsymbol{Z}}$ based on the three different approaches for the critical compressibility factor $Z_{c,SRK}$, $Z_{c,PR}$, $Z_{c,m}$ are shown in Fig. 2. Even at low temperatures above the triple point temperature, ammonia exhibits strong interactions owing to its polarity. The significant decrease in the compressibility factor with increasing temperature is a result of these interactions. Close to the critical temperature, the descriptions for the different compressibility factors deviate significantly from one another due to the differences of the critical compressibility factors. This results in an expected and inherently strong model insufficiency for the *SRK* or *PR* equation in the region of the critical point. The different estimated interaction parameters are shown in Table 4.

The application of Z modeling based on Eq. (13) to the vapor density description will now be discussed. To this end, the vapor density was calculated based on the critical compressibility factor $\boldsymbol{Z}_{c,m}$ and compared with the database from the VDI-Wärmeatlas (Fig. 3). The agreement between database and calculation is very good; the deviations up to the critical point are 0.5%. As expected, the critical density is calculated exactly for this model. The vapor density can be described up to the critical temperature.

In this context, Barile and Thodos (1965) proposed an empirical equation for calculating the vapor density where the reduced compressibility factor is expanded as a function of the vapor pressure and of the critical compressibility factor.

Table 4
Estimated coefficients and exponents for the compressibility factor of the ammonia vapor (Eq. (17)).

Parameter	Exp.	*SRK*	*PR*
Z_c	0.24268	0.3333	0.3074
$\hat{\boldsymbol{q}}_4$	5	5	5
$\hat{\boldsymbol{\Theta}}_{Z1}$	0.186608	0.0759525	0.110567
$\hat{\boldsymbol{\Theta}}_{Z2}$	−0.294962	−0.335347	−0.322714

Database: VDI-Wärmeatlas (2002, Dbf 5, Dcb 2). The critical compressibility factor $\boldsymbol{Z}_{c,m}$ is calculated from p_c,T_c,V_c. The basis is the model approach (13), (17)–(19) and $\boldsymbol{q}_1 = 200$, $\hat{\boldsymbol{\Theta}}_{Z3} = 0$.

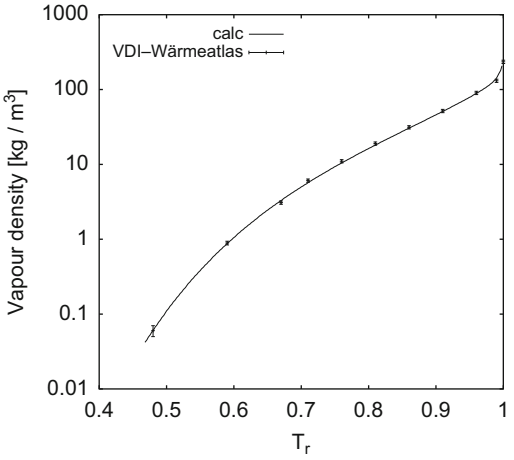

Fig. 3. Dependence of the NH_3 vapor density on the reduced temperature. •, Data from VDI-Wärmeatlas (2002, Dbf 5, Dcb 2). –, Estimator function according to Eqs. (13) and (17) where $\boldsymbol{Z}_{cm} = 0.243$. Validity range: $\boldsymbol{T}_r \in [0.482,1.0]$. The error bars show the standard deviation assumed with Eq. (3).

We calculated the vapor densities and the deviations from the measured and tabulated vapor density data in literature for the five compounds cited. For ammonia and chlorobenzene, the deviations are up to 4%, and for the remaining compounds up to 10%. These differences are too large for a kinetic model. The reason is probably that only vapor pressure terms occur in the reduced compressibility equation.

The characteristic compressibility factor for the vapor of each compound is the basis of the modeling of a CEoS on the dew line, which is discussed in the following section. Since vapor pressure and vapor density affect $\boldsymbol{Z}$, the trustworthiness of this parameter depends crucially on the measurement error of the vapor pressure and of the vapor density. For this reason, a validation of the model and its parameters is necessary. This is the subject of Section 6 of this study.

4. Application of Z modeling for the SRK and PR equation in the subcritical range

4.1. Definition of the Γ-function and of the Γ-CEoS

The information regarding the vapor pressure and the vapor density in the SRK and PR equation will now be taken into account. Instead of the $\boldsymbol{\alpha}$−function, we wish to define a $\boldsymbol{\Gamma}$−function such that it describes not the vaporization curve but the dew line in a temperature-dependent manner. To this end, in Eq. (1), the pressure is replaced by the estimator function of the vapor pressure $\hat{\boldsymbol{p}}_r$ according to Eq. (5), the molar vapor volume by the corresponding estimator function (13), and $\boldsymbol{\alpha}$ by $\boldsymbol{\Gamma}$. This gives rise to the $\boldsymbol{\Gamma}$−function for the dew line, which is then defined as follows:

$$\boldsymbol{\Gamma}_M := \frac{\boldsymbol{B}_M \boldsymbol{C}_M}{\Psi_M \hat{\boldsymbol{p}}_r} \cdot \left(\frac{\boldsymbol{T}_r}{\boldsymbol{A}_M} - 1 \right). \tag{20}$$

In this equation

$$\boldsymbol{A}_M = \hat{\boldsymbol{Z}}_M \boldsymbol{T}_r - \Omega_M \hat{\boldsymbol{p}}_r, \tag{21}$$

$$\boldsymbol{B}_M = \hat{\boldsymbol{Z}}_M \boldsymbol{T}_r + \delta_M \Omega_M \hat{\boldsymbol{p}}_r, \tag{22}$$

$$\boldsymbol{C}_M = \hat{\boldsymbol{Z}}_M \boldsymbol{T}_r + \varepsilon_M \Omega_M \hat{\boldsymbol{p}}_r. \tag{23}$$

This gives rise to the $\boldsymbol{\Gamma}$−SRK or $\boldsymbol{\Gamma}$−PR equation as a general equation of state:

$$p_M = \frac{RT}{\upsilon - b_M} - \frac{a_{c,M} \cdot \boldsymbol{\Gamma}_M(T)}{(\upsilon + \delta_M b_M) \cdot (\upsilon + \varepsilon_M b_M)}. \tag{24}$$

This equation describes, for the subcritical region, the pressure dependence on the molar volume and the temperature; in addition, the vapor pressure and the vapor density are described exactly for the dew line.

4.2. Properties of the Γ-function

First, the $\boldsymbol{\alpha}$−function and the $\boldsymbol{\Gamma}$−function are to be compared with one another. Fig. 4 shows the difference of these two functions for the SRK and PR equation. The correction taking account of vapor pressure and vapor density for the $\boldsymbol{\Gamma}$−function is significantly greater than for the $\boldsymbol{\alpha}$−function, which corrects only the vapor pressure. For less polar compounds, the two correction functions are virtually identical. What is also noticeable is the clear difference in the $\boldsymbol{\Gamma}$−function for the two equations of state. In order to calculate equal vapor densities with the two equations of state, a significantly greater correction is needed for the SRK equation.

In the VLE modeling of mixtures based on a $\gamma-\varphi$−approach, the virial equation is frequently used to describe the vaporous state. The difference of the $\boldsymbol{\Gamma}$−CEoS and of the virial equation can best be shown by a comparison of the virial coefficients of the two equations. To this end, the $\boldsymbol{\Gamma}$−CEoS is represented via Taylor expansion in a similar form to the virial equation. Proceeding from (24), the equation

$$Z_M = 1 + \sum_{k=1}^{\infty} \left[1 + \frac{a_{c,M} \boldsymbol{\Gamma}_M [(-\delta_M)^k - (-\varepsilon_M)^k]}{(\delta_M - \varepsilon_M) b_M \mathcal{R} T} \right] \cdot \left(\frac{b_M}{\upsilon} \right)^k \tag{25}$$

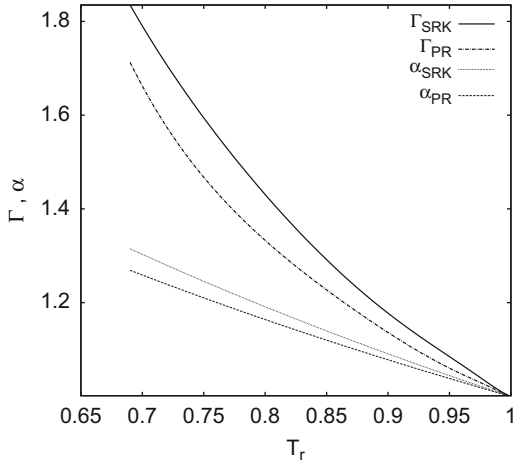

Fig. 4. Comparison of the $\boldsymbol{\alpha}$−function and $\boldsymbol{\Gamma}$−function for the SRK and PR equation for ammonia. The vapor density rises with rising correction values. The reduced triple point temperature is 0.482.

is obtained. Truncation after the 1st term of the Taylor series gives the 2nd coefficient $\boldsymbol{B}_{\Gamma,M}$

$$\boldsymbol{B}_{\Gamma,M} = b_M - \frac{a_{c,M}\boldsymbol{\Gamma}_M}{\mathcal{R}T} \tag{26}$$

of the $\boldsymbol{\Gamma}-$CEoS, which has a similar sense to the 2nd virial coefficient of the virial equation. For ammonia, $\boldsymbol{B}_{\Gamma,M}$ (Fig. 5), for temperatures below about $T_r < 0.85$, shows a very good agreement with the 2nd virial coefficient of the virial equation. Above $T_r > 0.85$, differences arise as expected, which have the causes already discussed in Section 3.1 and Appendix B. A further difference arises from the fact that the cubic SRK or PR equation possesses only one 2nd term, and the properties of the 2nd and 3rd virial coefficients in this 2nd term are described together, thus making an exact distinction between them impossible.

The difference in the $\boldsymbol{\Gamma}-$SRK and the virial equation is shown by the results of the vapor density calculation for ammonia. For it we calculated the points of intersections of the $p\upsilon$—trajectories with the real dew line at 116 °C, see Fig. 6 and Table 5. The state variables calculated by the virial equation show, as expected, a big difference to the real behavior. If the reference state, however, is

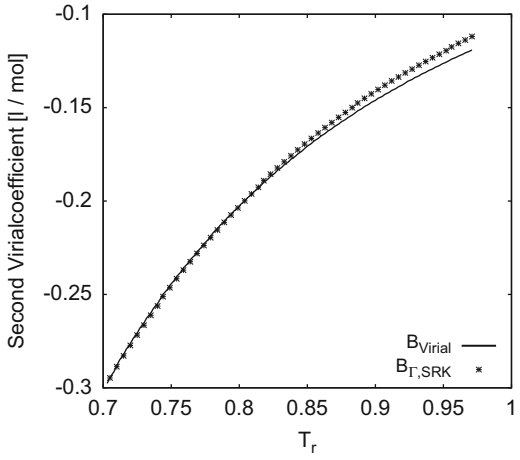

Fig. 5. Temperature dependence of the 2nd virial coefficient B_{Virial} of ammonia and the coefficient $\boldsymbol{B}_{\Gamma,M}$ of the $\boldsymbol{\Gamma}-$SRK equation.

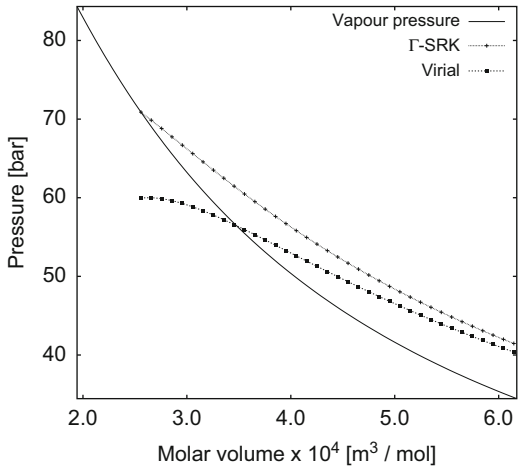

Fig. 6. Calculation of the molar vapor volume for ammonia by the virial equation and the $\boldsymbol{\Gamma}-$SRK equation. –, Dew line for the vaporous state in the temperature interval $\vartheta \in [72\,^\circ\text{C}, 116\,^\circ\text{C}]$ or $\boldsymbol{T}_r \in [0.85, 0.96]$. +, $p\upsilon-$graph for the $\boldsymbol{\Gamma}-$SRK equation at 106.5 °C ($\boldsymbol{T}_r = 0.936$). ■,($p\upsilon-$graph for the virial equation at 106.5 °C. The real properties are shown in Table 5.

Table 5
Comparison of the virial equation and $\boldsymbol{\Gamma}-$SRK with the real properties.

	Virial	$\boldsymbol{\Gamma}-$SRK	Real
Vapor pressure (bar)	~56.5	70.89	70.89
Molar vapor volume ($m^3/mol \times 10^4$)	~3.47	2.558	2.558

The parameters of the 2nd virial coefficient can be found in Appendix C. The temperature is 106.5 °C ($\boldsymbol{T}_r = 0.936$). The real vapor pressure and vapor density in shown in Ahrendts and Baehr (1979) or can be calculated by Eq. (5) and the parameter in Table 16.

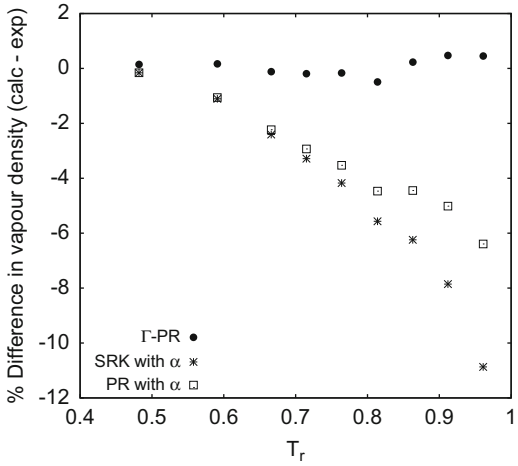

Fig. 7. Percentage deviation of the NH_3 vapor density calculation for different equations of state.

the dew line itself—as is the case for $\boldsymbol{\Gamma}-$EoS—the modeling of the molar vapor volume is ensured.

In summary, it can be stated that the virial equation must be checked for the vaporous state, and the $\Gamma-$EoS for the gaseous state. Both states are important because the fugacity coefficient, as an integral equation, also takes into account the gaseous state, and thus plays an important role in the VLE modeling. It is thus insufficient that only one state is well-described; the gaseous state and the vaporous state have to be well-described. The checking of the $\Gamma-$EoS for the gaseous state is described in detail in Section 4.4.

As expected, vapor density calculations based on a $\Gamma-$EoS are more accurate than the calculations with a CEoS based on an α correction function. Fig. 7 shows the comparison of the two equations of state with the different corrections. For comparison, the $\Gamma-$PR equation, which is somewhat better than the $\Gamma-$SRK equation, was selected. The $\Gamma-$PR equation is very significantly superior to both CEoS based on the $\alpha-$function.

Cubic equations of state are usually used within a VLE description ($\varphi-\varphi-$approach) both for the liquid phase and for the vapor phase. The prerequisite for this is that the Maxwell criterion (Maxwell equal area relation) is satisfied. Since the CEoS, according to Eq. (24), is defined only for the dew line and the liquid density is not taken into account, it does not satisfy the Maxwell equal area relation. Therefore the following inequation is valid:

$$\boldsymbol{p}\cdot(\upsilon_g - \upsilon_f) - \int_{\upsilon_f}^{\upsilon_g}\left[\frac{RT}{V-b_M} - \frac{a_{c,M}\cdot\boldsymbol{\Gamma}_M(T)}{(V+\delta_M b_M)\cdot(V+\varepsilon_M b_M)}\right]dV \neq 0. \tag{27}$$

This means that the $\Gamma-$EoS according to Eq. (24) must not be used for the combined modeling of vapor–liquid equilibria of both

phases, but only for the vapor phase. Γ−EoS cannot be used for the liquid phase description either.

4.3. Statistical confidence interval of the Γ-function

For the Γ−function, an error calculation based on the assumed measurement error with regard to vapor pressure and vapor density was carried out according to Eqs. (2) and (3), and the result shows, in Fig. 8, the confidence interval of the individual value. As expected, an enlargement in the 95% confidence interval is obtained with falling temperature, since the relative experimental error for the vapor pressure and vapor density measurement rises. The trustworthy temperature range is within the interval of $T_r \in [0.7,0.96]$ and, owing to measurement inaccuracies, is significantly smaller than the range of definition of the vapor pressure and vapor density database from the VDI-Wärmeatlas (2002, Dcb2). Minimizing the confidence interval is the topic of Section 6.

4.4. Predictive power of Γ−SRK and Γ−PR for the subcritical state

The Γ−EoS expanded to eleven data points each (VDI-Wärmeatlas, 2002, Dcb 2) for vapor pressure and vapor density in (24) is examined hereinafter for predictive power with regard to the description of the gaseous state of ammonia. The predictive power is examined using the difference of calculated pressure and the measured data of Beattie and Lawrence (1930), and Meyers and Jessup (1925). For the statistical evaluation, it is assumed that the measurement $p_{m,i}$ is a random sample with the stochastic error ε_i

$$p_{m,i} = p_i + \varepsilon_i, \quad \varepsilon_i \sim \mathcal{N}(0,\sigma^2) \tag{28}$$

and that the random error has standard distribution. Here, p_i means the true, unknown value. The measurements according to Beattie and Meyers are affected by a relative error v_i, and the standard deviation is calculated for the i-th measurement point according to

$$s_i = p_{m,i} \cdot v_i, \quad v_i \in \mathbb{R}^+. \tag{29}$$

Beattie and Lawrence (1930) give 0.08% and Meyers and Jessup (1925) give 0.155% for the relative error v_i. The predictive power is assessed as the "weighted sum of squares", WSS, according to the equation

$$WSS_M = \sum_{i=1}^{\mathcal{N}_m} \left(\frac{p_{M,i} - p_{m,i}}{s_i} \right)^2. \tag{30}$$

The greater the agreement between model and measurement, the smaller is WSS_M. For comparison, the quantity AAD% (absolute average deviation %) frequently cited in the literature

$$AAD\%_M = \frac{100}{\mathcal{N}_m} \sum_{i=1}^{\mathcal{N}_m} \left| \frac{p_{M,i} - p_{m,i}}{p_{m,i}} \right| \tag{31}$$

is also used.

For the comparison, the virial equation after truncation of the 2nd virial coefficient is also employed. The results of the comparative calculations (Table 6) show that the Γ−PR equation best describes the pVT measured data. The Γ−SRK equation is significantly worse, but much better than the virial equation. The greatest deviations are discernible in the low pressure range. Perhaps there are also adsorption phenomena which have not yet been corrected for completely in the low pressure range. The adsorption corrections are discussed in detail by Ahrendts and Baehr (1979, p. 11).

When the AAD% is employed for evaluation, the differences between the Γ−PR and the Γ−SRK are only small, even though the description of the Γ−PR is significantly better. The low AAD% magnitudes also suggest, in the virial equation, small deviations which are entirely satisfactory. Although the evaluation gives the same ranking as the WSS, it appears that the differences are not so serious and not worthy of discussion. Weighted sum of squares WSS is significantly more sensitive as a statistical evaluation parameter than AAD%, since the weighted squares are variances in the statistical sense and hence possess high significance. When information about the standard deviations of measured data is available or estimable, it is advisable to employ the WSS_M calculation to assess the predictive power.

It can be stated in summary that the Γ−EoS (24) modeled on the dew line can also calculate the gaseous state in advance, and hence possesses a high predictive power. Γ−PR is preferable to Γ−SRK in the case of ammonia.

4.5. Consistent description of caloric measurements with the Γ−PR equation

With an EoS, it is possible also to calculate caloric properties. They can be obtained via the residual properties function, i.e. the real part of an equation of state. Here we selected the specific heat capacity $\boldsymbol{C}_p$ of ammonia for the vaporous state. The calculations are to be done with Γ−PR, since it can be used to describe the vaporous and gaseous states very well. For comparison, the PR equation based on the α correction is also used for calculation. Both PR calculations are checked for a consistent description, by comparing the $\boldsymbol{C}_p$ measured data from the study by Barthau and Sohns (1974) and the data calculated from the VDI-Wärmeatlas (2002, Dcb 2) with the fundamental equation. The statement of a predictive power according to

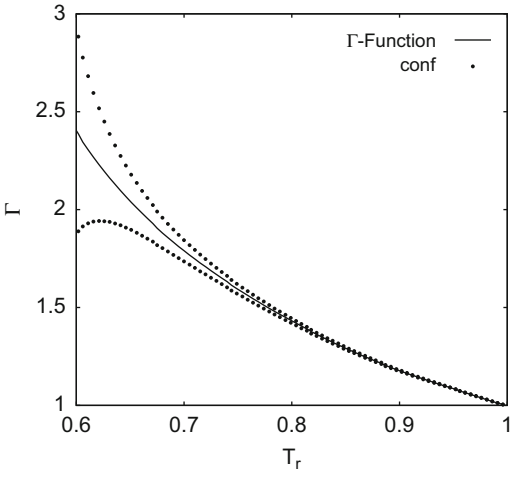

Fig. 8. Γ_{SRK}−function with 95% confidence intervals (•••) for ammonia based on error propagation of experimental variances.

Table 6
Predictive power of the Γ−EoS for the subcritical gaseous state.

EoS	WSS	AAD%
Γ−SRK	2480	0.24
Γ−PR	314	0.12
Virial	3090	0.66

Comparison of the model calculations with the measured data of Beattie and Meyers. $\mathcal{N}_m = 99$, $T_r \in [0.58,0.98]$, $v_r \in [4.7,305]$, $p_r \in [0.0078,0.607]$.

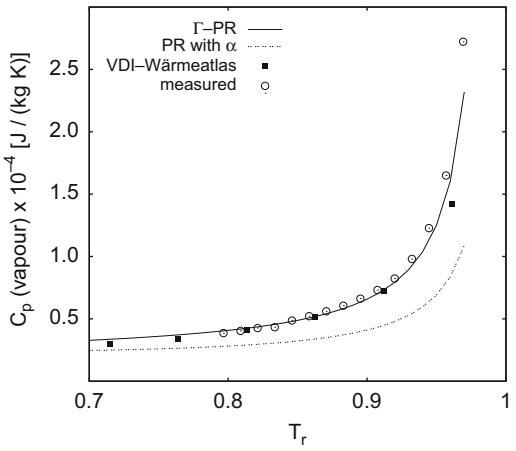

Fig. 9. Prediction of C_p vapor calculated with Γ–PR and the PR equation with α correction. In comparison: ○, Measured data of Barthau and Sohns (1974). ■, Tabulated data from the VDI-Wärmeatlas (2002, Dcb 2), calculated with the fundamental equation.

Table 7
Differences between the calculated, measured and tabulated heat capacities of ammonia vapor.

	Γ–PR	PR with α
AAD%	4.2	27
$r_{\min}$ (%)	−9	−50
$r_{\max}$ (%)	15	−18

Eq. (30) is not possible, since there is no information about the measurement error of $\boldsymbol{C}_p$. Consequently, the prediction is to be made via the specification of the AAD% according to Eq. (31), which, however, can only be considered as a very rough estimate in terms of quality. The specific heat capacity for both PR variants is calculated by the equation

$$\boldsymbol{C}_{p,M}(\boldsymbol{T}) = C_{p,id}(\boldsymbol{T}) - \int_{\upsilon}^{\infty} \left(\frac{\partial^2 p_M}{\partial T^2}\right)_V dV - R - \boldsymbol{T} \cdot \frac{\left(\frac{\partial p_M}{\partial T}\right)_{\upsilon}^2}{\left(\frac{\partial p_M}{\partial V}\right)_T}. \tag{32}$$

The temperature-dependent molar vapor volume υ is determined from Eq. (13) and, for $C_{p,id}(\boldsymbol{T})$, the equation specified in the publication by Barthau and Sohns (1974) is used. It can be seen from Fig. 9 that Γ–PR best describes the specific heat capacity and hence provides a consistent description of pVT measurements and caloric measured data. The detailed evaluation is shown in Table 7. The PR equation with the α correction exhibits a mean error AAD% of 27% in the specific heat capacity; Γ–PR is distinctly superior at 4.2 AAD%.

5. Modeling in the supercritical temperature range

To complete the description of the Γ–PR and Γ–SRK equation, the supercritical temperature range for NH_3 is also to be considered. The Γ–function is fitted directly using the tabulated data from the VDI-Wärmeatlas (2002, Dbf 5) based on the fundamental equation. Parameters for the Γ–SRK are $\Theta_\Gamma = (30.1573\ \ -50.8655\ \ 20.6385\ 1)^\top$, and $\Theta_\Gamma = (5.99154\ \ -11.5626\ \ 4.6409\ 1)^\top$ for the Γ–PR. The calculated pressures are compared with the measured data of Beattie and Lawrence (1930) and Meyers and Jessup (1925). The virial equation is used again for the comparative calculations. Table 8

Table 8
Predictive power of the Γ–EoS for the supercritical state of ammonia.

EoS	WSS	AAD%
Γ–SRK	966	0.15
Γ–PR	392	0.11
Virial	33 800	0.89

Comparison of the model calculations with the measured data of Beattie and Meyers. $\mathcal{N}_m = 144$, $T_r \in [1.04,1.47]$, $\upsilon_r \in [3.7,241]$, $p_r \in [0.014,1.17]$.

shows that the Γ–PR better describes the supercritical state better than the Γ–SRK equation and much better than the virial equation. Here again, the evaluation by means of AAD% on the basis of the low numerical value of 0.89% suggests a good description of the measurements, even though this is not the case.

6. Validation of the Γ-function and of the Γ -EoS

An EoS describes, for a pure substance, the relationship between pressure, molar volume and temperature $p = p(\upsilon,T,\Theta)$. The molecular interactions are specified by the parameter vector Θ. When the parameters are inaccurate, the state variables p,υ,T calculated therefrom are also inaccurate. The aim is to have reliable parameter values in order to obtain reliable values of the state variables in simulations. The Γ–function therefore has to be validated.

We briefly explain the principle of model-based experimental design, which is the basis for model validation. Since no new measurements can be carried out, values computed from the fundamental equation are assumed to be true, perturbed by a random error and treated as measurement data. These simulated measurements are used to validate the model.

6.1. Model-based experimental design

The model responses for the measurements η_i of pressure (and density, respectively) can be described as a function F of the particular reduced temperature T_{ri} and the model parameters $\Theta \in \mathbb{R}^{\mathcal{N}_\Theta}$ by a nonlinear relationship:

$$\eta_i = F(T_{ri},\Theta) + \varepsilon_i, \quad i = 1,\ldots,\mathcal{N}_m, \tag{33}$$

with normally distributed measurement errors $\varepsilon_i \sim \mathcal{N}(0,\sigma_i^2)$. To estimate the parameters from experimental data, nonlinear least squares problems have to be solved (Seber and Wild, 1989):

$$\min_{\Theta} \sum_{i=1}^{\mathcal{N}_m} \frac{(\eta_i - F(T_{ri},\Theta))^2}{\hat{s}_i^2}. \tag{34}$$

Here $\hat{s}_i$ are estimates for the standard deviations σ_i. Since the data are perturbed by measurement errors, the parameter estimate also has a statistical uncertainty which can be described by the variance–covariance matrix $\mathrm{Cov} \in \mathbb{R}^{\mathcal{N}_\Theta \times \mathcal{N}_\Theta}$, whose main diagonal elements are approximations for the variances of the parameters (Bock, 1987).

$$\mathrm{Cov} = (\mathrm{Jac}^\top \mathrm{Jac})^{-1} \text{ with } \mathrm{Jac}_{ij} = -\frac{1}{\hat{s}_i}\left(\frac{dF}{d\Theta_j}(T_{ri},\hat{\Theta})\Big|_{\Theta=\hat{\Theta}}\right)_{\substack{i=1,\ldots,\mathcal{N}_m \\ j=1,\ldots,\mathcal{N}_\Theta}}. \tag{35}$$

The variance–covariance matrix and hence the reliability of the estimate depends on the measurement error and the method of processing of the underlying experiments. In optimum experimental design, the experimental settings are computed such that the variance–covariance matrix of the estimate resulting from the data of these experiments is as small as possible in a quality criterion ϕ. The mathematical formulation of this problem leads

to nonlinear constrained optimization problems. In our case, experiments are designed by choosing the reduced temperature. As optimality criterion, we use the trace of the variance–covariance matrix. The experimental design problem is

$$\min_{T_{ri},i=1,\ldots,\mathcal{N}_m} \text{trace}(\text{Cov}) \quad \text{s.t. } \text{Cov}=(\text{Jac}^{\top}\text{Jac})^{-1}, \quad \text{Jac}_{ij}=-\frac{1}{s_i}\left(\frac{dF}{d\Theta_j}(T_{ri},\Theta)\right)_{\substack{i=1,\ldots,\mathcal{N}_m\\ j=1,\ldots,\mathcal{N}_\Theta}}. \tag{36}$$

Θ here is a guess for the values of the parameters. s_i are guesses for the $\hat{s}_i$. After evaluation of the optimized experiments, these values can change. In this case, experimental design and parameter estimation should be performed sequentially; see Körkel et al. (1999).

Mathematical methods and the software package VPLAN to solve these problems numerically, especially for nonlinear differential equation models, are discussed by Körkel (2002). A general overview over methodology and applications is given by Franceschini and Macchietto (2008) in a review article.

6.2. Multiple setpoint experimental design

In this study, nonlinear models $F^k(T_{ri},\Theta^k)$ of various scenarios $k=1,\ldots,K$ are considered, e.g. different chemical compounds or the different approaches of the Z_c modeling are in Section 3.2. In each of these scenarios, different substance- or model-specific values of parameters and constants enter the equations. In general, experimental designs for nonlinear models depend on the parameter values. In order to be able to propose generally valid experiments, here we use the new approach of *multiple setpoint experimental design*: we optimize an averaged criterion on the particular variance–covariance matrices of the individual scenarios, in this particular case the sum of the traces:

$$\min_{T_{ri},i=1,\ldots,\mathcal{N}_m} \sum_{k=1}^{K} \text{trace}(\text{Cov}^k) \tag{37}$$

$$\text{s.t. } \text{Cov}^k=(\text{Jac}^{k^{\top}}\text{Jac}^k)^{-1}, \quad \text{Jac}^k_{ij}=-\frac{1}{s^k_i}\left(\frac{dF^k}{d\Theta^k_j}(T_{ri},\Theta^k)\right)_{\substack{i=1,\ldots,\mathcal{N}_m\\ j=1,\ldots,\mathcal{N}_{\Theta^k}}}, \quad k=1,\ldots,K. \tag{38}$$

This experimental design problem corresponds to a parameter estimation, in which all parameters Θ^k of the individual scenarios are estimated from the same experiments:

$$\min_{\Theta^1,\ldots,\Theta^K} \sum_{k=1}^{K}\sum_{i=1}^{\mathcal{N}_m} \frac{(\eta^k_i-F^k(T_{ri},\Theta^k))^2}{\hat{s}^{k2}_i}. \tag{39}$$

This is because the variance-covariance matrix of the estimate $\hat{\Theta}_1,\ldots,\hat{\Theta}_K$ is then

$$\text{Cov}=\begin{pmatrix} \text{Cov}^1 & 0 & 0\\ 0 & \ddots & 0\\ 0 & 0 & \text{Cov}^K \end{pmatrix} \tag{40}$$

and the trace is the sum of the traces of Cov^k. For other optimality criteria, such as determinant or largest eigenvalue, the product of the determinants is used, or the maximum of the largest eigenvalues of the Cov^k. This method is now applied to the DIPPR equation.

6.3. Model validation of the DIPPR vapor pressure equation

The DIPPR vapor pressure equation (55) in the Appendix D is a semi-empirical equation with five parameters. With knowledge of the substance-specific constants p_c and T_c, the DIPPR equation can be rearranged to Eq. (5), where one of the parameters is replaced by the substance specific constant p_c. The integer exponent is 1 or 2 for many compounds, and can be assumed in each case as a constant for parameter estimation and experimental design. The vapor pressure equation (5) thus has three parameters Θ_{p1}, Θ_{p2} and Θ_{p3}. The parameter values for the compounds considered here are shown in Table 16 (Appendix D) and arise from a parameter estimation on the basis of literature data. To characterize the temperature-dependent vapor pressure of a compound, usually between 20 and 40 measurement points are collected. We want to find out whether we can use experimental design to reduce the number with approximately equal reliability of the parameters. First, an experimental design is to be calculated for ammonia. The reduced temperature $T_r\in[0.48,1]$ is chosen as control variable. We want to design an experimental series with the minimum number of measurements. In order that sufficient degrees of freedom still exist from a statistical point of view, six measurements are proposed as a minimum for the three unknown parameters. The lower temperature bound with an experiment at $T_r=0.48$ is fixed. The maximum temperature as the model limit is already included in the model with knowledge of the critical temperature T_c. It is thus possible to optimize five experiments. The proposed parameter values used are specified in Table 16 (Appendix D). The calculation yields only two optimal measured temperatures (Table 9) with repeated measurements.

If this experimental design were to be implemented, the following standard deviations would arise in the estimation of the parameters:

$$\Theta_{p1}=4625.45\pm 23,$$

$$\Theta_{p2}=-11.148\pm 0.16,$$

$$\Theta_{p3}=0.0162002\pm 0.00028. \tag{41}$$

The result shows that six experiments are sufficient to limit the uncertainty in the parameters to less than 5%.

In order to study the robustness of the experimental design with respect to different parameter values of several compounds, we calculated a *multiple setpoint experimental design* for all five compounds. For these too, the same optimal experiments are proposed as specified in Table 9. For the different compounds, the standard deviations shown in Table 10 would arise in the case of a parameter estimation. The experimental design specified in

Table 9
Optimal measurement temperatures for pressure measurements for the rearranged DIPPR vapor pressure Eq. (5).

T_r	Number of measurements
0.48	1
0.58	2
0.87	3

Model-based experimental design for the parameters Θ_{p1}, Θ_{p2}, Θ_{p3}.

Table 10
Standard deviations of the parameters of the DIPPR vapor pressure equation for an estimation with data from the optimized experiments.

	$\Theta_{p1,\text{new}}$	$\Theta_{p2,\text{new}}$	$\Theta_{p3,\text{new}}$
Ammonia	4625 ±23	−11.14 ±0.16	0.01620 ±0.00028
Hydrogen chloride	5395 ±19	−26.05 ±0.16	0.04911 ±0.00026
Sulfur dioxide	5580 ±24	−15.05 ±0.16	0.02105 ±0.00026
Chlorbenzene	7482 ±36	−11.69 ±0.16	0.01039 ±0.00018
Acetone	1716 ±29	8.70 ±0.16	−0.01028 ±0.00022

Table 9 is therefore valid for these and probably also many other compounds.

For model validation, new vapor pressure measurements are required for the optimal temperatures. In the course of this study, it was not possible to perform any measurements. The measurements were therefore simulated for ammonia by computations from the fundamental equation, see Ahrendts and Baehr (1979, p. 33, Table A), and perturbation with a stochastic relative error of 0.2%. These six simulated measurement points are then used to compute a new parameter estimate. Subsequently, the vapor pressure equation (5) and the newly estimated parameters are used to calculate the vapor pressures for 20 virtually equidistant temperatures, which are compared to the "true" values from the fundamental equation. For the critical pressure, the original value according to Ahrendts and Baehr (1979, p. 33, Table A) of 113.33 bar was used.

The new values of the vapor pressure parameters and standard deviations after the new estimation are

$$\Theta_{p1,\mathrm{new}} = 4817 \pm 35,$$

$$\Theta_{p2,\mathrm{new}} = -12.48 \pm 0.23,$$

$$\Theta_{p3,\mathrm{new}} = 0.01846 \pm 0.00039. \quad (42)$$

The weighted sum of squares WSS rounded to four digits is 1.406 and the corresponding value of the chi-square distribution $\chi^2_{0.99,3}$ for a confidence interval of 99% is 11.3. For model acceptance, WSS must not be greater than the corresponding threshold value of the chi-square distribution. This is the case and the model is therefore accepted and validated.

As a conclusion, it can be stated that, for the DIPPR vapor pressure equation, even six measured temperatures are sufficient for a model validation. Large measurement series of 20 and more measured temperatures are not necessary, and hence measurement time and costs are saved. The experimental design is valid for five different polar compounds and is probably also valid for many other compounds.

6.4. Model validation of the vapor density equation

The vapor density equation (13) based on $\boldsymbol{Z}$ modeling according to Eq. (17) is to be validated. We assume that the vapor pressure equation has been validated before. Θ_{z1} and Θ_{z2} are the parameters to be estimated. All other substance-specific parameters are considered as constants, see Tables 4 and 16. Again, the reduced temperature $T_r \in [0.48, 0.96]$ serves as a control variable. We have designed a series of ten experiments, one of which with T_r fixed at 0.48 and one with T_r fixed at 0.96. As a result of the optimum experimental design, repeated experiments are proposed; see Table 11. For this experimental design, the following standard deviations of the parameters are obtained:

$$\Theta_{Z1} = 0.1866 \pm 0.0048,$$

$$\Theta_{Z2} = -0.294 \pm 0.032. \quad (43)$$

Table 11
Optimal temperatures for density measurements for the vapor density equation (13).

T_r	Number of measurements
0.48	1
0.75	8
0.96	1

Model-based experimental design for parameters Θ_{z1}, Θ_{z2}.

As multiple setpoint scenario, we consider the parameter values which arise from the different modeling variants for Z_c (Table 4). The multiple setpoint experimental design results in the same experiments; see Table 11. The resulting parameter uncertainties are shown in Table 12.

Multiple setpoint experimental design for all five compounds also provides these optimal experiments and the standard deviations of the parameters shown in Table 13.

The optimal experimental design is thus robust to different approaches for Z_c and to different compounds. Repeated measurements are proposed. In order to further reduce the mean errors in the parameters, further repetitions are necessary, the mean error being inversely proportional to the root of the number of experiments.

For validation, we compute measurement pseudo-data with the aid of the FE table (Ahrendts and Baehr, 1979, p. 33, Table A) for this experimental design, perturb them with normally distributed errors with standard deviation 0.5% (for the repeated experiments of course, independently as often as required) and re-estimate the parameters from these data. For ammonia, this gives the new values

$$\Theta_{Z1,\mathrm{new}} = 0.1864 \pm 0.0048,$$

$$\Theta_{Z2,\mathrm{new}} = -0.162 \pm 0.032. \quad (44)$$

The comparison of a simulation of the model equations based on these values with the values from the FE table gives rise to a very good agreement; see Table 14. Our modeling results in a very

Table 12
Standard deviations of the parameters of the vapor density equation (13) resulting from the optimized experiments: comparison of the different approaches for Z_c.

	Θ_{Z1}	Θ_{Z2}
$Z_{c,m}$ (our approach)	0.1866 ±0.0048	−0.294 ±0.032
Z_c for PR	0.1105 ±0.0053	−0.322 ±0.035
Z_c for SRK	0.0759 ±0.0055	−0.335 ±0.037

Table 13
Standard deviations of the parameters of the vapor density equation (13) resulting from the optimized experiments: comparison of the different compounds.

	Θ_{Z1}	Θ_{Z2}
Ammonia	0.1866 ±0.0049	−0.294 ±0.032
Hydrogen chloride	0.1693 ±0.0051	0.661 ±0.040
Sulfur dioxide	0.2170 ±0.0054	−0.494 ±0.035
Chlorobenzene	0.2290 ±0.0055	−0.697 ±0.035
Acetone	0.3503 ±0.0045	−1.388 ±0.018

Table 14
Comparison of the values $\varrho(calc)$ calculated from the validated model (13) based on (17) with the values from the FE table $\varrho(FE)$ of ammonia.

Temp. (K)	$\varrho(calc)$ (kg/m^3)	$\varrho(FE)$ (kg/m^3)	AD%	WR
198.15	0.0787	0.0775	1.47	2.94
213.15	0.2151	0.2125	1.26	2.52
233.15	0.6522	0.6445	1.20	2.40
253.15	1.6216	1.6043	1.07	2.15
273.15	3.4869	3.4555	0.91	1.82
293.15	6.7441	6.6975	0.70	1.40
313.15	12.095	12.026	0.57	1.15
333.15	20.636	20.490	0.72	1.43
353.15	34.316	33.888	1.26	2.53
373.15	57.167	56.085	1.93	3.86
388.15	85.917	85.077	0.99	1.97

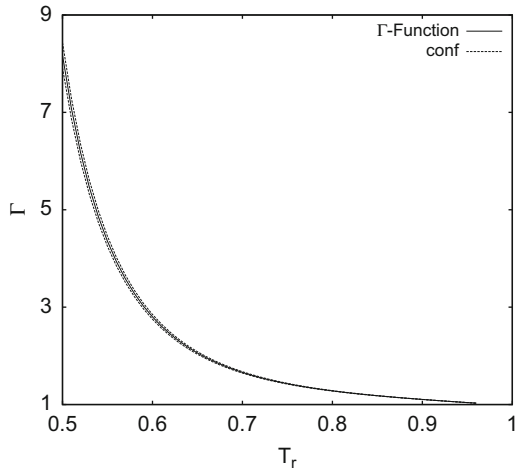

Fig. 10. Validated Γ−function with 95% confidence region for ammonia based on error propagation of the variance–covariance matrix of the parameters.

good description of the behavior of the compounds along the line of coexistence and is good enough for industrial applications.

6.5. Confidence interval of the Γ-function and of the Γ equation of state

We can now use the validated model equations to calculate the 95% confidence interval for the gamma-function. To this end, the method of "Unscented Transformation" was used as the basis, which is described in more detail by Julier et al. (2004). Basis of the error propagation to the Γ−function are the variance–covariance matrices and the estimated parameters of the $\hat{Z}$ function. The lower and upper 95% confidence intervals of the Γ−function for the PR equation can be found in Fig. 10. The maximum deviation at a reduced temperature of 0.5 is $\pm 3.16\%$. The validated confidence interval decreases with increasing temperature and has become significantly smaller compared to the invalidated Γ−function in Fig. 8. This reduction is attributable to the model-based experimental design. The random error for the gas and vapor density can now be calculated for the Γ−PR equation. For a requested error of $\pm 0.75\%$ in vapor density, the lower reduced temperature limit is about 0.57. The Γ−PR equation has now been validated for the requested maximum error in the temperature range [0.57, 0.96].

7. Summary

The α correction function for the *SRK* or *PR* equation does not describe the vapor density well enough for polar compounds. When this α correction function is calibrated to the gas density, high errors can occur in the case of extrapolation to the vapor density. Therefore, the dew line was used for the parameter assignment. Vapor density and vapor pressure serve to describe the compressibility factor $\boldsymbol{Z}$ of the dew line ($\boldsymbol{Z}$ modeling).

$\boldsymbol{Z}$ modeling is the basis of the correction function in the cubic equation of state. The correction function defined on the dew line is the Γ−function and the CEoS obtained therefrom is the Γ−EoS. The pVT properties for the gaseous state of ammonia calculated with the Γ−EoS agree very well with the measurements. For ammonia, the Γ−PR equation is better than the Γ−SRK equation, and both equations are significantly superior to the virial equation. This is of significance for kinetic modeling in which a VLE description is required. The reliability of estimated kinetic parameters is increased significantly as a result, since no considerable mass balance errors are projected into the kinetic parameters in a parameter estimation.

The Γ−PR equation is additionally validated using measured data of the specific heat capacity of the vapor. A comparison of the calculated heat capacities with measurements for ammonia shows that the mean deviations are about 4%. When, in contrast, the PR equation with the α correction function is used, the mean deviation is about 27%.

The Γ−EoS cannot be employed for the liquid phase description, since the Maxwell criterion is not met. Therefore, the application of the Γ−EoS in conjunction with VLE modeling of mixtures is recommended only for the $\gamma-\varphi$−approach.

For the validation of the model approach and parameters, model-based design of experiments is used. In order to obtain a uniform design for many compounds, the experimental design problem was extended for various parameter sets by so-called multiple setpoint optimization. For several given polar compounds, a uniform test plan was calculated for the DIPPR vapor pressure equation, which is also valid for ammonia. Only six temperature settings from the triple point temperature up to the critical temperature are needed for validation. For the vapor density estimator function, two parameters were validated. Here too, multiple setpoint optimization was employed to calculate the optimal measurement temperatures. VLE descriptions of mixtures are based on the pure substance properties and, therefore, apart from the vapor pressure and the liquid density, the vapor density should also be measured, since usually not all equations of state are calibrated sufficiently accurately for the vapor density.

Model-based design of experiments should serve as an addition to theoretical or complex empirical model approaches, in order that the risk of a systematic deviation (bias) between model and experiment is recognized. Instead of large measurement series a few measured data should be collected, but under the optimally designed conditions and with maximum experimental accuracy.

The application of Z modelling in the Γ−CEoS for mixtures has not been studied in this paper. We will try some common mixing rules, e.g. the geometric mean, and apply methods for model discrimination and model validation. If the *pVT* properties are described very well, the caloric properties will arise as a good result. The mixing rules have to be validated by optimum experimental design and by experimental data of the vapor density and the corresponding composition.

Notation

Subscript indices, symbols

g	gaseous phase, rich: vapor
f	liquid phase
m	measured
M	model

Superscript indices, symbols

(0)	substance-based property (*e.g.* pure substance vapor pressure)
$\top$	transposed of a matrix
-1	inverse of a matrix
$\hat{}$	estimated parameter

Constants

$\mathcal{R}$	gas constant = 8.314472 [J/(mol·K)]
$\mathcal{M}$	molar mass of a compound [kg/mol]

T_c	crit. temperature of a compound [K]
p_c	crit. pressure of a compound [bar]
v_c	crit. molar volume of a compound [l/mol]
T_p	triple point temperature, K
b_M	constant in the CEoS
δ_M	constant in the CEoS
ε_M	constant in the CEoS
Ω_M	constant in the CEoS
Ψ_M	constant in the CEoS
$a_{c,M}$	constant for the attraction term in the cubic EoS [N·m^4/mol^2]

Variables, state variables and functions (equilibrium state: in bold type)

ϑ	temperature [°C]
T	absolute temperature [K]
T_r	reduced temperature for a pure substance $T_r=T/T_c$
ω	acentric factor, Pitzer factor
ϱ^*	molar pure substance density [mol/l]
ϱ	pure substance density [kg/l]
υ	molar volume of the pure substance [l/mol]
υ_r	reduced molar volume of the pure substance
p	pressure [bar]
p_r	reduced pressure $p_r=p/p_c$
p_m	measured pressure [bar]
Z	compressibility factor for a compound
$\tilde{\boldsymbol{Z}}$	approximation of $\boldsymbol{Z}$
$\hat{\boldsymbol{Z}}$	estimator function of $\boldsymbol{Z}$
$Z_{\mathrm{Vir},k}$	virial coefficient k of the virial equation expressed in Z
$\boldsymbol{p}^{(0)}$	pure substance vapor pressure of the compound [bar]
$\hat{\boldsymbol{p}}$	estimator function of the pure substance vapor pressure of the compound [bar]
B	2nd virial coefficient [l/mol]
$\hat{B}$	estimator function for the 2nd virial coefficient [l/mol]
α	alpha-function, vapor pressure correction function in the cubic EoS for a compound, dimensionless
Γ	gamma-function, vapor pressure and vapor density correction function in the cubic EoS, dimensionless
$\boldsymbol{A}_M,\boldsymbol{B}_M,\boldsymbol{C}_M$	functions for definition of the gamma-function, dimensionless
q	exponent in the estimator function $\hat{\boldsymbol{Z}}$
Jac	Jacobi matrix
F	general function

Statistical parameters

s	standard deviation of the measurement
s^2	variance of the measurement
σ^2	variance of a normal distribution with all samples
v	coefficient of variation = standard deviation/mean, also relative error of a measurement
$\mathcal{N}$	number, in general
$\mathcal{N}$	number of measurement points
$\mathcal{N}_m$	number of estimated parameters
$\mathcal{N}_\Theta$	number of estimated parameters
ε	random error ($\varepsilon_i \sim \mathcal{N}(0,\sigma_i^2)$)
η	measurement in general
$\mathcal{N}$	normal distribution
$\chi^2_{1-(\alpha/2),\mathcal{N}_m-\mathcal{N}_\Theta}$	threshold value or limit of significance of the chi squared distribution with the error probability α and the degree of freedom $\mathcal{N}_m-\mathcal{N}_\Theta$
$\boldsymbol{\Theta}_M$	parameter vector of a model
$\hat{\boldsymbol{\Theta}}_M$	estimated parameter vector of a model
Σ	diagonal matrix of the variances of the individual measurements diag($s_1^2,s_2^2,\ldots,s_{\mathcal{N}_m}^2$)
Cov	variance-covariancematrix
r_i	residuum i, difference between estimated and measured value
WR	with standard deviation weighted residual
WSS	weighted sum of squares

Numbers

$\mathbb{N}$	set of natural numbers; $i,k,n \in \mathbb{N}$
$\mathbb{R}$	set of real numbers

Abbreviations

AAD%	Average Absolute Deviation Percent
AD%	Absolute Deviation Percent AD% $=\lvert($ model $-$measurement)/measurement $\rvert \cdot 100$
CEoS	Cubic Equation of State, specifically in this publication SRK and PR equations
DIPPR	Design Institute for Physical Properties
EoS	Equation of State
FE	Fundamental Equation based on Helmholtz energy
PR	Peng-Robinson
SRK	Soave-Redlich-Kwong
VdW	Van der Waals
VLE	Vapor-Liquid Equilibrium
$\gamma-\varphi$	approach to the description of a vapor-liquid equilibrium (VLE); liquid phase with an activity coefficient model and the vapor phase with a fugacity coefficient approach

Acknowledgements

The authors give their sincere thanks for the valuable discussions with Dr. Anna Schreieck, Dr. Eckhard Ströfer, Dr. Hergen Schultze and Dr. Armin Bader from BASF SE.

Appendix A

Model parameters for the SRK and PR equations are summarized in Table 15.

The molecularly specific constants $a_{c,M}$ and b_M are calculated according to

$$a_{c,M} = \Psi_M \frac{(\mathcal{R}T_c)^2}{p_c}, \tag{45}$$

$$b_M = \Omega_M \frac{\mathcal{R}T_c}{p_c}, \tag{46}$$

$$\alpha_{SRK}(T) = [1+(0.48+1.574\omega-0.176\omega^2)\cdot(1-\sqrt{T/T_c})]^2, \tag{47}$$

$$\alpha_{PR}(T) = [1+(0.37464+1.54226\omega-0.26992\omega^2)\cdot(1-\sqrt{T/T_c})]^2. \tag{48}$$

Appendix B

Here the difference between the Z-functions $\boldsymbol{f}_z(\boldsymbol{T},\Theta_Z)$, $\tilde{\boldsymbol{f}}_z(\boldsymbol{T},\Theta_Z)$ (Eqs. (9) and (11)) and the virial equation is be discussed, since this equation is based on a similar expansion. To this end, we consider the equation of state f_z' as a function of the molar density $\varrho^* = 1/\upsilon$, the temperature and the molecular interaction parameters Θ_Z, Θ_Z' and write

$$f_z'(\varrho^*,T,\Theta_Z') := f_z\left(\frac{1}{\varrho^*},T,\Theta_Z\right) = f_z(\upsilon,T,\Theta_Z) = Z. \tag{49}$$

$f_z'(\varrho^*,T,\Theta_Z')$ can likewise be expanded according to Taylor at the point ϱ_0^*

$$f_z'(\varrho^*,T,\Theta_Z') = \sum_{k=0}^{\infty} \frac{(\varrho^*-\varrho_0^*)^k}{k!} \cdot \left(\frac{\partial^k f_z'(\varrho^*,T,\Theta_Z')}{\partial \varrho^{*k}}\right)_{\varrho_0^*}. \tag{50}$$

If the coefficients in (50) are considered, which are identical to the virial coefficients $B(T,\Theta_B)$, $C(T,\Theta_C)$, etc.

$$Z_{\mathrm{Vir},1} = B(T,\Theta_B) := \lim_{\varrho_0^*\to 0}\left(\frac{\partial f_z'(\varrho^*,T,\Theta_Z')}{\partial \varrho^*}\right)_{\varrho_0^*}, \tag{51}$$

$$Z_{\mathrm{Vir},2} = C(T,\Theta_C) := \lim_{\varrho_0^*\to 0}\frac{1}{2!}\left(\frac{\partial^2 f_z'(\varrho^*,T,\Theta_Z')}{\partial \varrho^{*2}}\right)_{\varrho_0^*}, \tag{52}$$

one obtains for $\varrho_0^* = 0$ and with (49), the known form of the virial equation

$$Z = \sum_{k=0}^{\infty} \frac{(\varrho^*)^k}{k!} \cdot Z_{\mathrm{Vir},k}(T,\Theta_Z). \tag{53}$$

The two expansions (11) and (53) differ in the following aspects:

- The virial equation describes the subcritical gaseous state, the vaporous state and the supercritical state as a function of the variables ϱ^* or υ and T. For this purpose, however, the knowledge of an infinitely large number of virial coefficients is needed.
- The compressibility factor in Eq. (11) applies only for the dew line in the vapor–liquid equilibrium as a function of only one independent variable, the temperature.
- For the coefficients of the virial equation, the reference state is the limit for the density tending to zero. For the expansion of the saturation compressibility factor according to (9) or (11), the reference state is the temperature-dependent vapor density and an arbitrarily selected temperature $\boldsymbol{T}_0$ in the temperature range of $\boldsymbol{T}_{\boldsymbol{p}} \le \boldsymbol{T}_0 < T_c$.

Table 15
Model parameters for the SRK and PR equations of state.

M	δ_M	ε_M	Ω_M	Ψ_M	$Z_{c,M}$
SRK	0	1	$\frac{2^{1/3}-1}{3}$	$\frac{1}{9(2^{1/3}-1)}$	1/3
PR	$1-2^{1/2}$	$1+2^{1/2}$	0.077796	0.457235	0.307401

Appendix C

Second virial coefficient for ammonia.

The temperature dependence of the 2nd virial coefficient is known from a study by Djordjevic and Mihajlov-Dudukovic (1980, pp. 858-862). The parameters of an approximation function for the 2nd virial coefficient were fitted to the results of Djordjevic and Mihajlov-Dudukovic (1980, p. 860, Fig. 2: the calculated curve). The virial equation thus fitted was used to carry out the $\rho\upsilon$ calculations for ammonia. The estimator function used for the 2nd virial coefficient was the equation

$$\hat{B}(T_r,\hat{\Theta}_B) = \hat{\Theta}_{B1} + \hat{\Theta}_{B2}\cdot e^{(\hat{\Theta}_{B3}/T_r)} + \hat{\Theta}_{B4}\cdot e^{(\hat{\Theta}_{B5}/T_r)} \tag{54}$$

in [l/mol] with the parameters $\hat{\Theta}_B = (0.00401974\ 0.0777724\ 0.99266\ -0.0699288\ 1.53413)^{\top}$. The range of validity for the temperature is likewise specified there.

Appendix D

Table 16 gives an overview of the substance data used in this study. Literature sources for the substance-specific data T_c, p_c, T_{p_r}, Z_c for the compounds originate from the following works:

NH_3	Ahrendts and Baehr (1979, p. 9)
HCl	VDI-Wärmeatlas (2002, Dca 1, Dcb 6), Ahlberg (1985, pp. 342–353), Landold-Börnstein (1960, part a, p. 189), vapour density data for $\vartheta \ge 0\,^{\circ}$C
SO_2	VDI-Wärmeatlas (2002, Dca 1) and Walas (1985, p. 163)
CH_3COCH_3	VDI-Wärmeatlas (2002, Dcb 2)
C_6H_5Cl	VDI-Wärmeatlas (2002, Dca 1, Da 11)

The parameters $\hat{\Theta}_p$ in Table 16 originate from a parameter estimation based on vapor pressure measurements from the references cited. A relative error of 1% was assumed for the parameter estimation, since no statement is made about the statistical error. The entire DIPPR compilation is regressed with the modified Riedel equation and is called the DIPPR equation no. 101

$$\hat{\boldsymbol{p}} = \exp\left[A + \frac{B}{\boldsymbol{T}} + C\cdot\ln(\boldsymbol{T}) + D\cdot\boldsymbol{T}^E\right]. \tag{55}$$

Table 16
Characteristic properties of the compounds used in this study.

	NH_3	HCl	SO_2	CH_3COCH_3	C_6H_5Cl
T_c (K)	405.55	324.6	430.8	508.15	632.4
p_c (bar)	112.8	83.09	78.834	47.61	45.2
T_{p_r}	0.48	0.487	0.435	0.349	0.359
Z_c	0.24268	0.249	0.27022	0.2397	0.265
Acentric factor ω	0.25	0.131	0.245	0.306	0.25
$\hat{\Theta}_{p1}\times 10^{-3}$	4.62546	5.39513	5.58018	1.7161	7.48174
$\hat{\Theta}_{p2}$	−11.1481	−26.0506	−15.0536	8.7028	−11.6864
$\hat{\Theta}_{p3}\times 10^{2}$	1.62002	4.91064	2.10524	−1.0279	1.0392
$\hat{\Theta}_{p4}$	1	1	1	1	1
Scope for T_r	0.48–0.96	0.7–0.95	0.46–0.96	0.66–0.94	0.59–0.93

A rearrangement of this equation with knowledge of the critical temperature and of the critical pressure leads to Eq. (5). Only three estimated parameters thus remain and the parameter estimation problem is significantly better conditioned with regard to "overfitting". Table 16 reports the parameter values for the scaled equation (5).

References

Ahlberg, K., 1985. AGA Gas Handbook. AGA AB Lidingö, Sweden.

Ahrendts, J., Baehr, H.D., 1979. VDI-Forschungsheft 596.

Baehr, H.D., Tillner-Roth, R., 1995. Thermodynamische Eigenschaften umweltverträglicher Kältemittel. Springer Verlag, Berlin.

Barile, R.G., Thodos, G., 1965. Saturated vapor and liquid densities of pure substances. The Canadian Journal of Chemical Engineering, 137–142.

Barthau, G., Sohns, J., 1974. Thermische Eigenschaften von Ammoniak. Chemie Ingenieur Technik 46 (4) synopse MS 019/74.

Beattie, J.A., Lawrence, C.H., 1930. Some of the thermodynamic properties of ammonia. The Journal of the American Chemical Society 52 (6).

Bock, H.G., 1987. Randwertproblemmethoden zur Parameteridentifizierung in Systemen nichtlinearer Differentialgleichungen. Bonner Mathematische Schriften, vol. 183. Universität Bonn, Bonn.

Djordjevic, B.D., Mihajlov-Dudukovic, A.N., 1980. American Institute of Chemical Engineering 26 (5).

Franceschini, G., Macchietto, S., 2008. Model-based design of experiments for parameter precision: state of the art. Chemical Engineering Science 63, 4846–4872.

Julier, S.J., Uhlmann, J.K., Jeffrey, K., 2004. Unscented filtering and nonlinear estimation. Proceedings of the IEEE 92 (3), 401–422.

Körkel, S., 2002. Numerische Methoden für optimale Versuchsplanungsprobleme bei nichtlinearen DAE-Modellen. Ph.D. Thesis, Universität Heidelberg, Heidelberg.

Körkel, S., Bauer, I., Bock, H.G., Schlöder, J.P., 1999. A sequential approach for nonlinear optimum experimental design in DAE systems. In: Keil, F., Mackens, W., Voss, H., Werther, J. (Eds.), Scientific Computing in Chemical Engineering II, vol. 2. Springer-Verlag, Berlin, Heidelberg, pp. 338–345.

Landold-Börnstein, 1960. Bd. II, 6. Auflage, 2. Teil, Bandteil a. Springer-Verlag, Berlin, Göttingnen, Heidelberg. Publisher Klaus Schäfer and Ellen Lax.

Meyers, C.H., Jessup, R.S., 1925. The specific volume of superheated ammonia vapor. Refrigerating Engineering 11, 345–354.

Perry, R.H., Green, D.W., 1997. Perry's Chemical Engineers' Handbook, seventh ed.

Poling, B.E., Prausnitz, J.M., O'Connell, J.P., 2001. The Properties of Gases and Liquids, fifth ed. McGraw-Hill, New York. ISBN 0-07-011682-2.

Prausnitz, J.M., Lichtenthaler, R.N., Azevedo, E.G., 1999. Molecular Thermodynamics of Fluid-Phase Equilibria, third ed. Prentice Hall, New Jersey. ISBN 0-13-977745-8.

Sandurasi, J.A., Kidnay, A.J., Yesavage, V.F., 1986. Compilation of parameters for a polar fluid Soave–Redlich–Kwong equation of state. Industrial & Engineering Chemistry Process Design and Development 25, 957–963.

Seber, G.A.F., Wild, C.J., 1989. Nonlinear Regression. John Wiley & Sons, New York, Chichester, Brisbane, Toronto, Singapore. ISBN 0-471-61760-1.

Smith, J.M., Ness, H.C.V., Abbott, M.M., 2005. Introduction to Chemical Engineering Thermodynamics, seventh ed. Mc Graw-Hill, New York. ISBN 007-124708-4.

Soave, G., 1972. Equilibrium constants from a modified Redlich–Kwong equation of state. Chemical Engineering Science 27, 1197–1203.

Soave, G., 1979. Institution of Chemical Engineers Symposium Series 56, 1.2/1.

Tillner-Roth, R., Harms-Watzenberg, F., Baehr, H.D., 1993. DKV-Tagungsbericht 20 (II/1), 167–181.

Twu, C.H., Bluck, D., Cunningham, J.R., Coon, J.E., 1991. A cubic equation of state with a new alpha function and a new mixing rule. Fluid Phase Equilibria 69, 33–50.

Twu, C.H., Sim, W.D., Tassone, V., 2002. Getting a handle on advanced cubic equations of state. Chemical Engineering Progress 98 (11), 58–65.

VDI, 2002. Verein Deutscher Ingenieure VDI-Gesellschaft Verfahrenstechnik und Chemieingenieurwesen, VDI-Wärmeatlas, ninth ed. Springer.

Walas, S.M., 1985. Phase Equilibrium in Chemical Engineering. Butterworth Publishers, Stoneham, MA. ISBN 0-409-95162-5.